European Congress on Computational Methods in Applied Sciences and Engineering
ECCOMAS Computational Fluid Dynamics Conference 2001
Swansea, Wales, UK, 4-7 September 2001

NUMERICAL MODELLING SUBSONIC AND SUPERSONIC INDUCTIVE PLASMA FLOWS

Sergei V. Utyuzhnikov[†*], Andrei V.Konyukhov*, Denis V.Rudenko*,

Sergei A. Vasil'evskii, Anatolii F. Kolesnikov** and G.S.R. Sarma*****

† Department of Mechanical Engineering, UMIST, P.O. Box 88, Manchester, M60, 1QD, UK, e-mail: s.utyuzhnikov@umist.ac.uk

* Moscow Institute of Physics and Technology, Dolgoprudny 141700, Russia

** Institute for Problems in Mechanics in RAS, 101 Prospect Vernadskogo, Moscow

*** DLR, Institute fur Stromungsmechanik, Bunsen str. 10, D-37073 Gottingen, Germany

Key words: Plasmatron, Navie-Stokes equations, low Mach number flows, high temperatures, TVD schemes.

Abstract. *A physico-chemical model, numerical method and computation results for equilibrium inductive coupled plasma flows in a plasmatron are presented. Numerical solutions of the Navier-Stokes equations coupled with a quasi-1D approximation of the Maxwell equations for stationary laminar axisymmetric flows with swirling have been obtained. A new effective preconditioning technique along with an implicit TVD scheme is used to solve the Navier-Stokes equations in both subsonic and supersonic regimes. To simulate the flow the full Navier-Stokes equations are written in the cylindrical coordinate system with account for three velocity components - axial, radial and tangential component due to the flow spinning, together with energy equation written for the total gas enthalpy. The equations include source terms corresponding to the electromagnetic field influence: the Lorentz force components (so called, magnetic pressure) and Joule heat production. The necessary transport coefficients were calculated in advance for equilibrium plasma as the functions of pressure and temperature. Transport properties were calculated by the precise formulae of the Chapman-Enskog method in temperature range $300 \le T \le 15000$ K for five gases: air, nitrogen, oxygen, argon, carbon dioxide. Calculations of equilibrium air, nitrogen, oxygen, argon and carbon dioxide plasma flows for the IPG-4 (IPM, Moscow) discharge channel geometry with the channel radius $Rc = 0.04$ m and length $Zc = 0.46$ m were performed. Two codes were developed to carry out the calculations. The first code (code 1) is based on the SIMPLE algorithm with the under-relaxation procedure for improving stability. The time-relaxation method along with the implicit scheme and preconditioning is used in the second code (code 2) .*

1 INTRODUCTION

A modern application of the inductively coupled plasmas is simulating thermochemical interaction of high-enthalpy gas flows with thermal protection materials (TPM) at the hypersonic flight conditions[1-4]. The IPG plasmatrons at IPM RAS appeared to be very efficient tools for the TPM aerothermal testing, and the prediction of the TPM catalycity[1,2]. The efficient capabilities of the 100-kW IPG-4 plasmatron for the simulation of physico-chemical processes accompanying the hypersonic entry of a vehicle aeroshell in the Martian atmosphere have been demonstrated recently[5,6]. But in fact, the potential capabilities of R&D facilities to simulate reacting flow physics and real surface processes can be revealed, if the measurements are properly combined with CFD modeling. CFD modeling is an indispensable tool for aerothermal testing in order to carry out CFD codes validation, to rebuild flow field in plasmatron and to extract TPM catalycity related to atoms recombination from heat transfer measurements. In general, the problem is rather tricky. Up to now there are few computations of the nonequilibrium air plasma flow coupled with the RF electromagnetic field[7].

The philosophy of CFD modeling developed at IPM consists in the separation of the whole flow field into plasmatron in three computation zones, where the distinctive flow features can be used for the efficient approach[6]. For the plasmatron operating conditions the general CFD problem is divided in the three problems as follows:

1. the equilibrium inductively coupled swirling plasma flow within the cylindrical discharge channel;
2. the equilibrium subsonic axisymmetric high-enthalpy laminar jet flow past a cylindrical model;
3. the nonequilibrium multicomponent boundary layer with the finite thickness at the stagnation point.

A new numerical algorithm presented and computer code have been developed to simulate the problem without dividing all domain into different subregions. The algorithm allows us to simulate both sub- and supersonic regimes in a unique manner.

In the paper we present the capabilities of CFD modeling inductively coupled plasmas and some results of computations carried out by two different codes in the wide range of the IPG-4 plasmatron operating conditions for different equilibrium plasmas (air, nitrogen, oxygen, carbon dioxide, argon). The advanced technology developed for calculations of the plasma transport coefficients based on the rigorous modification of the Chapman-Enskog formalism[8] and appropriate database for thermodynamic and transport properties are presented as well.

Two codes were used to carry out the calculations. The first code is based on the SIMPLE algorithm with the under-relaxation procedure for improving stability. The time-relaxation method along with the implicit scheme and preconditioning, is used in the second code. A comparison of both codes was done ealier[9]. A new approach how to use preconditioning techniques with TVD schemes is suggested. In the special case of the Roe scheme the method[10] is obtained. In[10] the particularities of the use of upwind schemes at low Mach numbers were considered for the first time where it was shown how the preconditioning technique can reveal the problems concerned with loosing accuracy at low Mach numbers.

2 GOVERNING EQUATIONS

Plasma flow in an induction plasmatron discharge channel under the LTE conditions is assumed to be governed by the Navier-Stokes equations for compessible gas (taking into account the Lorentz force and Joule heating) and the Maxwell equations for RF electromagnetic field. The gas dynamical subset of governing equations with the Joule heat source of the electric resistance and with the Lorentz force term is as follows:

$$\frac{\partial \boldsymbol{U}}{\partial t}+\frac{\partial(\boldsymbol{E^i}-\boldsymbol{E^v})}{\partial z}+\frac{\partial(\boldsymbol{G^i}-\boldsymbol{G^v})}{\partial r}+\boldsymbol{S}^i-\boldsymbol{S}^v=\boldsymbol{S}^e \tag{2.1}$$

$$\boldsymbol{U}=\begin{bmatrix}\rho\\ \rho u\\ \rho v\\ \rho w\\ E\end{bmatrix},\ \boldsymbol{E^i}=\begin{bmatrix}\rho u\\ \rho u^2+p\\ \rho uv\\ \rho uw\\ u(E+p)\end{bmatrix},\ \boldsymbol{G^i}=\begin{bmatrix}\rho v\\ \rho vu\\ \rho v^2+p\\ \rho vw\\ v(E+p)\end{bmatrix},\ \boldsymbol{S^i}=\frac{1}{r}\begin{bmatrix}\rho v\\ \rho vu\\ \rho(v^2-w^2)\\ 2\rho vw\\ v(E+p)\end{bmatrix}\ \boldsymbol{S^e}=\begin{bmatrix}0\\ 0\\ F_r^{\,l}\\ 0\\ Q^J\end{bmatrix}$$

$$\boldsymbol{E^v}=\begin{bmatrix}0\\ \tau_{zz}\\ \tau_{zr}\\ \tau_{z\theta}\\ \tau_{zz}u+\tau_{zr}v+\tau_{z\theta}w+\dfrac{\mu}{Pr}h_z\end{bmatrix},\ \boldsymbol{G^v}=\begin{bmatrix}0\\ \tau_{zr}\\ \tau_{rr}\\ \tau_{r\theta}\\ \tau_{zr}u+\tau_{rr}v+\tau_{r\theta}w+\dfrac{\mu}{Pr}h_r\end{bmatrix}$$

$$\boldsymbol{S^v}=\frac{1}{r}\begin{bmatrix}0\\ \tau_{zr}\\ \tau_{rr}-\tau_\theta\\ 2\tau_{r\theta}\\ \tau_{zr}u+\tau_{rr}v+\tau_{r\theta}w+\dfrac{\mu}{\mathrm{Pr}}h_r\end{bmatrix}$$

$$\tau_{zz}=\frac{2}{3}\mu\left(2\frac{\partial u}{\partial z}-\frac{\partial v}{\partial r}-\frac{v}{r}\right),\ \tau_{rr}=\frac{2}{3}\mu\left(2\frac{\partial v}{\partial r}-\frac{\partial u}{\partial z}-\frac{v}{r}\right),\ \tau_\theta=\frac{2}{3}\mu\left(2\frac{v}{r}-\frac{\partial u}{\partial z}-\frac{\partial v}{\partial r}\right)$$

$$\tau_{zr}=\mu\left(\frac{\partial u}{\partial r}+\frac{\partial v}{\partial z}\right),\ \tau_{r\theta}=\mu\left(\frac{\partial w}{\partial r}-\frac{w}{r}\right),\ \tau_{z\theta}=\mu\frac{\partial w}{\partial z}$$

$$E=\rho e+\rho\frac{u^2+v^2+w^2}{2},\quad h=e+\frac{p}{\rho}$$

The equations are written in a cylindrical coordinates (z,*r*) (z corresponds to the axial

coordinate, r - radial). Axial symmetry with non zero transversal momentum is assumed. Index 'i' corresponds to inviscid flux vectors and source terms and 'v' corresponds to the viscouse ones. The axial component of the Lorentz force is neglected.

The averaged Lorentz force and Joule heating term in the right hand side of (2.1) are expressed in the terms of the electric field which is assumed to be the sum of two contributions $E = E_V + E_P$, where E_V is induced by current in the inductor coil, while E_P is generated by vortical currents in plasma. E_V is calculated by means of the Biot-Savart law once before solving (2.1). The plasma-induced electric field amplitude E_P is governed by

$$\frac{\partial^2 E_P}{\partial z^2} + \frac{1}{r}\frac{\partial}{\partial r}\left(r\frac{\partial E_P}{\partial r}\right) - \frac{1}{r^2}E_P - i2\pi\mu_0\sigma f(E_V + E_P) = 0 \tag{2.2}$$

Unlike E_V, the plasma-induced electric field E_P is updated at each iteration or time step.

The governing equations are closed with constitutive relations which define electrical conductivity, transport properties and equation of state of plasma under LTE conditions. The equation of state, conductivity and transport properties are handled in a table form.

3 NUMERICAL APPROXIMATION OF THE HYPERBOLIC PART OF THE GOVERNING EQUATIONS BY IMPLICIT TVD SCHEME

A structured grid which is adaptive to the flow geometry is used. All metric information is expressed in the terms of finite volume method notations. The second order upwind TVD scheme, originally developed by Harten and Yee[11], is used to approximate flux vectors and flux vector Jacobian matrices at the cell faces. The scheme is based on local characteristic approach and has the second order of accuracy in space almost everywhere excepting extrema of the characteristic variables. The corresponding set of linear algebraic equations can be written in δ-form as

$$\left[\mathbf{I} + \frac{\tau}{Vol}\left(\sum_{k=1,4} < A - \frac{\partial \boldsymbol{F}_n^{\boldsymbol{v}}}{\partial \mathbf{V}}\frac{\partial \mathbf{V}}{\partial \boldsymbol{U}} >_k^n + Vol\cdot\left(\frac{\partial \mathbf{S}^i}{\partial \boldsymbol{U}} - \frac{\partial \mathbf{S}^v}{\partial \boldsymbol{U}}\right)\right)\right]\Delta\boldsymbol{U} = \tag{3.1}$$

$$-\frac{\tau}{Vol}\left(\sum_{k=1,4} < \boldsymbol{F}_n - \boldsymbol{F}_n^{\boldsymbol{v}} >_k^n + Vol\cdot(\mathbf{S}^i - \mathbf{S}^v - \mathbf{S}^e)\right)$$

where index k identifies one of cell faces {i-1/2, j; i+1/2, j; i, j-1/2; i, j+1/2}, brackets $< f >_k^n$ denote numerical approximation of function f at face k, $\boldsymbol{U} = (\rho, \rho u, \rho v, E)^T$ is the vector of the conservative variables, $\boldsymbol{V}=(p, u, v, h)^T$, $\Delta\boldsymbol{U} = \boldsymbol{U}^{n+1} - \boldsymbol{U}^n$, Vol is the volume of a cell, $\boldsymbol{F}_n^{\boldsymbol{v}} = n_x\boldsymbol{E}^{\boldsymbol{v}} + n_y\boldsymbol{G}^{\boldsymbol{v}}$ is a vector of viscous fluxes, $\vec{n} = (n_x, n_y)^T$ is an external normal vector to a cell face, $\frac{\partial \boldsymbol{F}_n^{\boldsymbol{v}}}{\partial \boldsymbol{V}} = n_x\frac{\partial \boldsymbol{E}^{\boldsymbol{v}}}{\partial \boldsymbol{V}} + n_y\frac{\partial \boldsymbol{G}^{\boldsymbol{v}}}{\partial \boldsymbol{V}}$ is an operator resulting from a linearization

of the viscous fluxes.

Numerical inviscid flux vector at face (i+1/2, j) is given by

$$< \boldsymbol{F_n} >^n_{i+1/2,j} = \frac{1}{2}(\boldsymbol{F_n}(\boldsymbol{n}_{i+1/2,j}, \boldsymbol{U^n_{i,j}}) + \boldsymbol{F_n}(\boldsymbol{n}_{i+1/2,j}, \boldsymbol{U^n_{i+1,j}}) + R_{i+1/2,j} \cdot \Phi_{i+1/2,j}) \tag{3.2}$$

The matrix $R_{i+1/2,j}$ represents the right eigenvectors of the Jacobian matrix $A(\boldsymbol{n},\boldsymbol{U})$ corresponding to the flux vector $\boldsymbol{F}_n(\boldsymbol{n},\boldsymbol{U})$.

The elements ϕ^l of vector Φ for the upwind TVD scheme are (the second index j is omitted everywhere for simplicity):

$$\phi^l_{i+1/2} = \frac{1}{2}\psi(a^l_{i+1/2})(g^l_i + g^l_{i+1}) - \psi(a^l_{i+1/2} + \gamma^l_{i+1/2})\alpha^l_{i+1/2}$$

where $a^l_{i+1/2}$ are the eigenvalues of the Jacobian matrix $A(\boldsymbol{n},\boldsymbol{U})$, $\alpha^l_{i+1/2}$ is approximates variation of the local characteristic variables at midpoints $\alpha^l_{i+1/2} = R^{-1}_{i+1/2}(\boldsymbol{U}^n_{i+1} - \boldsymbol{U}^n_i)$.

$$g^l_i = \min \mathrm{mod}(\alpha^l_{i-1/2}, \alpha^l_{i+1/2}),$$

$$\gamma^l_{i+1/2} = \frac{1}{2}\psi(a^l_{i+1/2})\begin{cases} \dfrac{(g^l_{i+1} - g^l_i)}{\alpha^l_{i+1/2}}, & \alpha^l_{i+1/2} \neq 0 \\ 0, & \alpha^l_{i+1/2} = 0 \end{cases}$$

The coefficient of numerical viscosity corrected to satisfy an entropy inequality is given by the formula[11]

$$\psi(\mathrm{z}) = \begin{cases} |z|, & |z| \geq \varepsilon \\ \dfrac{(z^2 + \varepsilon^2)}{2\varepsilon}, & |z| < \varepsilon \end{cases}$$

The approximation of the numerical flux Jacobian at the cell face (i+1/2,j), $< A >^n_{i+1/2,j}$, is obtained after a linearization of the numerical flux term given by (3.2)

$$< A >^n_{i+1/2,j} \Delta\boldsymbol{U_{ij}} = \frac{1}{2}(A(\boldsymbol{n}_{i+1/2,j}, \boldsymbol{U^n_{i,j}})\Delta\boldsymbol{U_{i,j}} + A(\boldsymbol{n}_{i+1/2,j}, \boldsymbol{U^n_{i+1,j}})\Delta\boldsymbol{U}_{i+1,j}$$
$$+ \Omega_{i+1/2,j}(\Delta\boldsymbol{U}_{i+1,j} - \Delta\boldsymbol{U_{i,j}})),$$
$$\Omega_{i+1/2,j} = R_{i+1/2,j} \cdot diag[\beta^l - \psi(a^l + \gamma^l)]_{i+1/2,j} \cdot R^{-1}_{i+1/2,j},$$

where

$$\beta^l_{i+1/2,j} = \frac{(g^l_{i,j} + g^l_{i+1,j})}{\alpha^l_{i+1/2,j}}$$

Values $a^{l}_{i+1/2,j}$ $R_{i+1/2,j}$, $R^{-1}_{i+1/2,j}$, are calculated by an averaging procedure of some kind.

Since an equation of state for reacting gas is used in the computations of plasma flow inside a plasmatron torch, a particular form of the functions of state should be used. The Jacobian matrices and the matrices of left and right eigenvectors for the case of an arbitrary equation of state are given below. The flux vector representing fluxes of conservative variables U through the cell face is

$$\boldsymbol{F}_n = \boldsymbol{F}\cdot\boldsymbol{n} = \begin{pmatrix} \rho\theta \\ \rho\theta u + n_x p \\ \rho\theta v + n_y p \\ \rho\theta(E+p) \end{pmatrix}, \quad \theta = \boldsymbol{V}\cdot\boldsymbol{n} = n_x u + n_y v$$

corresponding Jacobian matrix is

$$A = \begin{Vmatrix} 0 & n_x & n_y & 0 \\ -u\theta + n_x m_1 & \theta + n_x(u+m_2) & n_y u + n_x m_3 & n_x m_4 \\ -v\theta + n_y m_1 & n_x v + n_y m_2 & \theta + n_y(v+m_3) & n_y m_4 \\ \theta(m_1 - (E+p)\rho^{-1}) & n_x(E+p)\rho^{-1} + \theta m_2 & n_y(E+p)\rho^{-1} + \theta m_3 & \theta(1+m_4) \end{Vmatrix}$$

where $m_k = \dfrac{\partial p}{\partial U_k}$ can be expressed in terms of p_e, p_ρ as follows

$$m_1 = \left.\frac{\partial p}{\partial \rho}\right|_e + \frac{1}{\rho}\left.\frac{\partial p}{\partial e}\right|_\rho (u^2+v^2-\frac{E}{\rho}),\ m_2 = -\frac{u}{\rho}\left.\frac{\partial p}{\partial e}\right|_\rho,\ m_3 = -\frac{v}{\rho}\left.\frac{\partial p}{\partial e}\right|_\rho,\ m_4 = \frac{1}{\rho}\left.\frac{\partial p}{\partial e}\right|_\rho$$

The eigensystem decomposition of Jacobian matrix has the form $A = R^{-1} diag[\theta,\theta,\theta+\sigma a,\theta-\sigma a]R$, here a is the sound velocity, σ is the area of the face.

Matrices of the right and the left eigenvectors are given by

$$R = \begin{Vmatrix} 1 & 0 & \alpha & \alpha \\ u & \tilde{n}_y\rho & \alpha(u+\tilde{n}_x a) & \alpha(u-\tilde{n}_x a) \\ v & -\tilde{n}_x\rho & \alpha(v+\tilde{n}_y a) & \alpha(v-\tilde{n}_y a) \\ \Theta & (\tilde{n}_y u - \tilde{n}_x v)\rho & \alpha(\Phi+\Theta+a\tilde{\theta}) & \alpha(\Phi+\Theta-a\tilde{\theta}) \end{Vmatrix},$$

$$R^{-1} = \begin{Vmatrix} 1-\dfrac{\varphi^2}{a^2} & \dfrac{\Gamma u}{a^2} & \dfrac{\Gamma v}{a^2} & -\dfrac{\Gamma}{a^2} \\ -(\tilde{n}_y u - \tilde{n}_x v)\rho^{-1} & \tilde{n}_y\rho^{-1} & -\tilde{n}_x\rho^{-1} & 0 \\ \beta(\varphi^2 - a\tilde{\theta}) & \beta(\tilde{n}_x a - \Gamma u) & \beta(\tilde{n}_y a - \Gamma v) & \beta\Gamma \\ \beta(\varphi^2 + a\tilde{\theta}) & -\beta(\tilde{n}_x a + \Gamma u) & -\beta(\tilde{n}_y a + \Gamma v) & \beta\Gamma \end{Vmatrix},$$

where $\tilde{n}_x = \frac{n_x}{\sigma}, \tilde{n}_y = \frac{n_y}{\sigma}$ are the components of the unit normal , $\alpha = \frac{\rho}{a\sqrt{2}}, \beta = \frac{1}{\rho a\sqrt{2}}$,

$\tilde{\theta} = \tilde{n}_x u + \tilde{n}_y v$, $\Theta = \frac{E}{\rho} + \rho e_\rho|_p$, $\varphi^2 = m_1 = (0.5(u^2+v^2) - e - \rho e_\rho|_p)\Gamma$, $\Gamma = \frac{1}{\rho e_p|_\rho}$,

$\Phi = \rho e_p|_\rho \, a^2$, $a^2 = P_\rho|_e + \frac{p}{\rho^2} P_e|_\rho$, $e_p|_\rho = \frac{1}{P_e|_\rho}$, $e_\rho|_p = -\frac{P_\rho|_e}{P_e|_\rho}$

3.1 Preconditioning governing equation system

The gas flow inside a plasmatron discharge channel is characterized by a low Mach number (usually, 0.01 < M < 1). As well known, the governing equations become stiff as Mach number tends to zero and thus the convergence rate of the iteration procedure is slow. In recent years, a number of preconditioning methods have been developed by several authors to solve the problem[10]. The preconditioning matrix[10] has the simplest diagonal form $P = diag[\beta^2, 1, 1, 1]$ in the variables pressure - entropy $\boldsymbol{W} = (p, u, v, S)^T$. Here, β is a preconditioning parameter. Then the preconditioning matrix in conservative variables $\boldsymbol{U} = (\rho, \rho u, \rho v, E)^T$ is as follows

$$P_c = \frac{\partial \boldsymbol{U}}{\partial \boldsymbol{W}} P \frac{\partial \boldsymbol{W}}{\partial \boldsymbol{U}} = \frac{\partial \boldsymbol{U}}{\partial \boldsymbol{V}} \frac{\partial \boldsymbol{V}}{\partial \boldsymbol{W}} P \frac{\partial \boldsymbol{W}}{\partial \boldsymbol{V}} \frac{\partial \boldsymbol{V}}{\partial \boldsymbol{U}} \tag{3.3}$$

One can obtain an appearance of the preconditioning matrix in conservative variables for a gas with an arbitrary equation of state

$$P_c = \mathrm{I} + (\beta^2 - 1)\frac{\Gamma}{a^2} \begin{Vmatrix} -\frac{\varphi^2}{\Gamma} & u & v & -1 \\ -\frac{\varphi^2}{\Gamma} u & u^2 & vu & -u \\ -\frac{\varphi^2}{\Gamma} v & uv & v^2 & -v \\ -\frac{\varphi^2}{\Gamma}(E+p)\rho^{-1} & u(E+p)\rho^{-1} & v(E+p)\rho^{-1} & -(E+p)\rho^{-1} \end{Vmatrix}$$

where I is the unit matrix and

$\frac{\varphi^2}{\Gamma} = (\frac{1}{2}(u^2+v^2) - e - \rho e_\rho|_p)$, $\Gamma = \frac{1}{\rho e_p|_\rho}$, $e_p|_\rho = \frac{1}{p_e|_\rho}$, $e_\rho|_p = \frac{p_\rho|_e}{p_e|_\rho}$,

$$a^2 = p_\rho\,|_e + \frac{p}{\rho^2}\,p_e\,|_\rho$$

Instead of (3.1) we solve

$$\left[P_c^{-1} + \frac{\tau}{Vol}\left(\sum_{k=1,4} < A - \frac{\partial \boldsymbol{F_n}^{\boldsymbol{v}}}{\partial \boldsymbol{U}} >_k^n + Vol\cdot(\frac{\partial \boldsymbol{S}^i}{\partial \boldsymbol{U}} - \frac{\partial \boldsymbol{S}^v}{\partial \boldsymbol{U}})\right)\right]\Delta \boldsymbol{U} = \tag{3.4}$$

$$-\frac{\tau}{Vol}(\sum_{k=1,4} < \boldsymbol{F_n} - \boldsymbol{F_n}^{\boldsymbol{v}} >_k^n + Vol\cdot(\boldsymbol{S}^i - \boldsymbol{S}^v - \boldsymbol{S}^e))$$

But a TVD approximation is constructed in (3.4) as for the system

$$P_c^{-1}\frac{\partial \boldsymbol{U}}{\partial t} + \frac{\partial(\boldsymbol{E^i - E^v})}{\partial z} + \frac{\partial(\boldsymbol{G^i - G^v})}{\partial r} + \boldsymbol{S}^i - \boldsymbol{S}^v = \boldsymbol{S}^e$$

So that

$$< \boldsymbol{F_n} >_{i+1/2,j}^n = \frac{1}{2}(\boldsymbol{F_n}(\boldsymbol{n}_{i+1/2,j}, \boldsymbol{U}_{\boldsymbol{i,j}}^{\boldsymbol{n}}) + \boldsymbol{F_n}(\boldsymbol{n}_{i+1/2,j}, \boldsymbol{U}_{i+1,j}^n) + P_{c\,i+1/2,j}^{-1}\tilde{R}_{i+1/2,j}\cdot\tilde{\Phi}_{i+1/2,j})$$

$$< A >_{i+1/2,j}^n \Delta \boldsymbol{U}_{\boldsymbol{ij}} = \frac{1}{2}(A(\boldsymbol{n}_{i+1/2,j}, \boldsymbol{U}_{\boldsymbol{i,j}}^{\boldsymbol{n}})\Delta \boldsymbol{U}_{\boldsymbol{i,j}} + A(\boldsymbol{n}_{i+1/2,j}, \boldsymbol{U}_{i+1,j}^n)\Delta \boldsymbol{U}_{i+1,j} +$$

$$P_{c\,i+1/2,j}^{-1}\tilde{\Omega}_{i+1/2,j}(\Delta \boldsymbol{U}_{i+1,j} - \Delta \boldsymbol{U}_{\boldsymbol{i,j}})),$$

$$\tilde{\phi}_{i+1/2,j}^l = \frac{1}{2}\psi(\tilde{\alpha}_{i+1/2,j}^l)(\tilde{g}_{i,j}^l + \tilde{g}_{i+1,j}^l) - \psi(\tilde{\alpha}_{i+1/2,j}^l + \tilde{\gamma}_{i+1/2,j}^l)\tilde{\alpha}_{i+1/2,j}^l,$$

$$\tilde{\Omega}_{i+1/2,j} = \tilde{R}_{i+1/2,j}\cdot diag[\tilde{\beta}^l - \psi(\tilde{\alpha}^l + \tilde{\gamma}^l)]_{i+1/2,j}\cdot\tilde{R}_{i+1/2,j}^{-1},$$

where $\tilde{R}$ and $\tilde{\alpha}$ correspond to the right eigenvectors matrix and eigenvalues of the matrix P_cA accordingly.

It is easy to show that following this way it is possible to deduce the method obtained in[10] for the Roe scheme of the first order of approximation.

An approximate factorization method is applied to solve (3.4)

$$(P_c^{-1} + L_i + L_j)\Delta \boldsymbol{U} = RHS,$$

where L_i, L_j are the operators in the left hand side of (3.4) corresponding to different coordinate directions. An approximate factorization is as follows

$$(P_c^{-1} + L_j)P_c(P_c^{-1} + L_i)\Delta \boldsymbol{U} = RHS \tag{3.5}$$

Thus, the solution procedure at each iteration (or time step) consists of several steps

$$(P_c^{-1} + L_i)\Delta \boldsymbol{U}^{n+1/2} = RHS \tag{3.6}$$
$$(P_c^{-1} + L_j)\Delta \boldsymbol{U}^{n} = P_c^{-1}\Delta \boldsymbol{U}^{n+1/2}$$
$$\boldsymbol{U}^{n+1} = \boldsymbol{U}^{n} + \Delta \boldsymbol{U}^{n}$$

Numerical tests we have carried out reveal dramatic improvement in convergence rate provided preconditioner (3.3) is used. Test steady state calculations are performed for viscous flow in channels with adiabatic walls. Results shown in Fig. 1 and 2 correspond to $M_o=10^{-2}$, where M_o -is Mach number at the inlet of the chanell. The number of iterations required to diminish the norm of the residual to 10^{-6} is shown against CFL number for both the preconditioned and non preconditioned methods. In Fig. 2 the evolution of the residual norm at the given CFL number is presented.

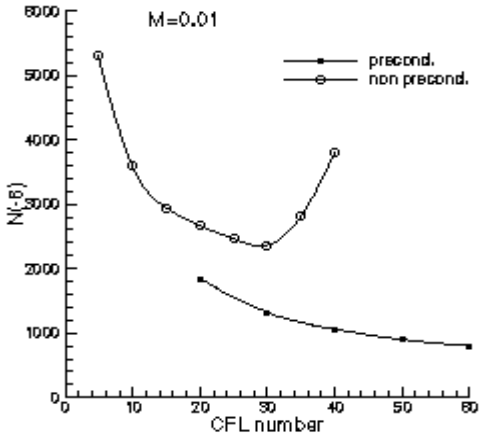

Figure 1.: Number of iterations required to diminish the norm of the residual to 10^{-6}

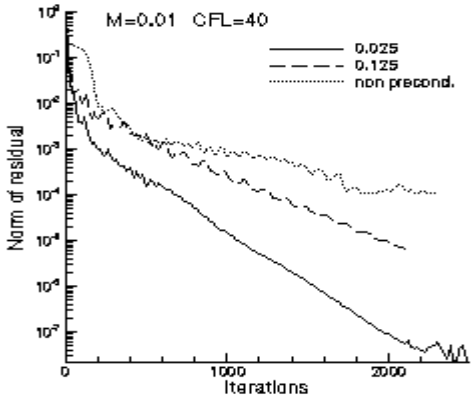

Figure 2.: Evolution of the norm of residual for different values of the preconditioning parameter

It should be noted that these results refer to the case when there is no external heating. If there are strong variations of density in the flow field the method demonstrates slow rate of convergence at extremely low Mach numbers and even fails in some cases. This behavior can be explained by the error of the pressure reconstruction at cell faces in the right hand side of equations. This error remains the same whether preconditioning is used or not. In the present technique, pressure is calculated at cell faces in terms of the conservative variables given at cell nodes via the equation of state $p = p(\rho, e)$. So, the pressure reconstruction error has the same order of magnitude as density and energy (temperature) have. At very low Mach number without heating, density is nearly constant. The relative variations of density and energy in the flow have order *O(M²)* hence the pressure reconstruction error is of the same order as the variations of a pressure in the flow field and the numerical method works well. If density and temperature vary not only due to compressibility but also due to strong heating and its variation is *O(1)* the pressure reconstruction error has order of magnitude *O(1)* while the pressure variation in the flow field remains *O(M²)*. To solve this problem one can obtain pressure at cell faces not from the equation of state but from the solution directly i.e. pressure must be one of the independent variables then pressure reconstruction error (thanks to an interpolation) is *O(M²)*. It is important to conserve numerical approximation in the right hand side of the governing equations at the same time. The modified method uses $\boldsymbol{V} = (p,u,v,h)^T$ as independent variables and the final approximation used is as follows:

$$\left[MP_v + \frac{\tau}{Vol} \sum_{k=1,4} < \overline{A} - \frac{\partial \boldsymbol{F}_n^{(v)}}{\partial \boldsymbol{V}} >_k^n \right] \Delta \boldsymbol{V} = -\frac{\tau}{Vol} \left(\sum_{k=1,4} < \boldsymbol{F}_n - \boldsymbol{F}_n^{v} >_k^n + Vol \cdot (\boldsymbol{S}^i - \boldsymbol{S}^v - \boldsymbol{S}^e) \right) \tag{3.7}$$

where

$$M = \frac{\partial \boldsymbol{U}}{\partial \boldsymbol{V}}, \; P_V = \frac{\partial \boldsymbol{V}}{\partial \boldsymbol{W}} P \frac{\partial \boldsymbol{W}}{\partial \boldsymbol{V}} \quad \overline{A} = AM = \frac{\partial \boldsymbol{F}}{\partial \boldsymbol{V}}$$

$$M = \begin{Vmatrix} \frac{1}{c^2} - \frac{1}{\rho} \rho_h |_p & 0 & 0 & \rho_h |_p \\ \left(\frac{1}{c^2} - \frac{1}{\rho} \rho_h |_p \right) u & \rho & 0 & \rho_h |_p \, u \\ \left(\frac{1}{c^2} - \frac{1}{\rho} \rho_h |_p \right) v & 0 & \rho & \rho_h |_p \, v \\ \left(\frac{1}{c^2} - \frac{1}{\rho} \rho_h |_p \right) (h + \frac{\mathbf{v}^2}{2}) - 1 & \rho u & \rho v & \rho_h |_p \, (h + \frac{\mathbf{v}^2}{2}) + \rho \end{Vmatrix}, \tag{3.8}$$

where

$$\frac{1}{c^2} = (\rho_p|_h + \frac{1}{\rho}\rho_h|_p),\ P_V = \begin{Vmatrix} \beta^2 & 0 & 0 & 0 \\ 0 & 1 & 0 & 0 \\ 0 & 0 & 1 & 0 \\ \frac{\beta^2 - 1}{\rho} & 0 & 0 & 1 \end{Vmatrix}$$

Unlike the original version described above, this modified formulation of implicit Harten-Yee scheme for an arbitrary equation of state given in the form $\rho = \rho(p,h)$ is found to be stable at all Mach numbers including extremely low ones.

4 EQUILIBRIUM DISCHARGE GASDYNAMICS & ELECTRODYNAMICS

We assume a subsonic flow in a cylindrical discharge channel is stationary, laminar and axisymmetric one with a swirl in azimuth direction. High frequency electromagnetic field does not influence gas transport properties, radiative processes are negligible and the flow is under LTE. To simulate the flow we use full Navier-Stokes equations written in cylindrical coordinate system with account for three velocity components - axial, radial and also tangential one due to the flow spinning, together with the energy equation written for the total gas enthalpy. These equations include source terms corresponding to electromagnetic field influence: Lorentz force components (so called magnetic pressure) and Joule heat production. Boundary conditions for Navier-Stokes equations are following: necessary flow parameters are specified at annular inlet slot at the channel entry section; velocity components equal zero at rigid surfaces; well known "soft" conditions are applied at the channel exit section; symmetry conditions are applied at the axis.

Suppose that oscillating external current in separate inductor circular coils produces a monochromatic electric field with complex amplitude $\vec{E}(z,r)$. Following Boulos[12] we use the assumption for tangential component of the electric field amplitude $E_\theta(z,r)$: $\partial E_\theta / \partial z << \partial E_\theta / \partial r$, that leads to quasi-1D approximation of Maxwell equations:

$$\frac{d}{dr}\left(\frac{1}{r}\frac{d}{dr}\left(rE_\theta\right)\right) = -i\omega\mu_0\sigma E_\theta\,, \qquad i\omega\mu_0 H_z = \frac{1}{r}\frac{d}{dr}\left(rE_\theta\right) \tag{4.1}$$

Here z and r are axial and radial coordinates; $\omega = 2\pi f$ is circular frequency of monochromatic electric field, σ is plasma electrical conductivity, μ_0 is vacuum magnetic permeance, H_z is complex amplitude of magnetic field axial component. In this approximation the axial component of Lorentz force equals zero. Obtained quasi-1D approximation is an essential simplification for the problem, it leads to a boundary value problem for the ordinary differential equation written above to determine the complex amplitude of vortical electric field $E_\theta(z,r)$; z coordinate is a parameter only in this equation, E_θ depends on z owing to boundary conditions. To determine E_θ we use also symmetry condition at the axis $E_\theta(z,0) = 0$ and the condition at the discharge channel wall[13,14] as follows:

$$r = R_c: \quad \frac{1}{r}\frac{d}{dr}\left(rE_\theta\right) = i\omega\mu_0 H_{zc0}(z) \qquad (4.2)$$

Here R_c is the channel radius, H_{z0} is the amplitude of magnetic field axial component at the channel wall produced by the inductor RF current outside the plasma flow. The comparison of the full two-dimensional Maxwell equations solutions with the quasi-1D approximation results presented in[15] showed a good accuracy of this approximation in a wide range of operating frequencies for the plasma torch geometry under consideration.

5 CALCULATION OF PLASMAS TRANSPORT PROPERTIES

To solve the Navier-Stokes and Maxwell equations, transport coefficients are necessary: viscosity, thermal conductivity and electrical conductivity. In our method transport coefficients were calculated in advance for the equilibrium plasma flows as functions of pressure and temperature. The effects of non-ideal gas and plasma were not accounted for. The transport properties were calculated by the precise formulae of Chapman-Enskog method[8] in the temperature range $300 \le T \le 15000$ K for different gases: air, nitrogen, oxygen, argon, carbon dioxide. Calculation technique and appropriate results for air transport properties under LTE were presented previously in[16]. The first non-zero approximation is rather accurate to calculate transport coefficients for neutral gases, but for ionized gases it can lead to ~50% error[16,17]. Our calculations for high temperatures were made with $\zeta = 2$ for viscosity, and $\zeta = 4$ for other transport coefficients to provide 5% accuracy, here ζ is the order of approximation by Sonine polynomials, i.e. number of terms in Sonine polynomial expansions of Boltzmann's equation solution that provide transposition in the Chapman-Enskog method. Exploited formulae[8] for transport properties are more convenient for calculations than the classic formulae[17,18] of Chapman-Enskog method, because the latter formulae are more complicated and use higher order determinants: $N\zeta \times N\zeta$ instead of $N(\zeta\text{-}1) \times N(\zeta\text{-}1)$.

Viscosity μ, effective heat conductivity λ_{eff} and electrical conductivity σ calculated in the 2-nd (μ) and 4-th approximation (λ_{eff} and σ) at P = 0.1 atm for the five gases are presented in Fig. 3-5. The curves for λ_{eff} show difference between argon (lower curve without any peaks at T<12000K) and the molecular gases with one (pure nitrogen and pure oxygen) or two (air and CO_2) peaks due to dissociation at T<12000K. Air electrical conductivity is higher than that of the other gases at low temperatures: $3000 \le T \le 6000$ K. But at higher temperatures $6000 \le T \le 15000$ K carbon dioxide electrical conductivity is higher than that of the other gases, though in this temperature range the difference between electrical conductivity of air, nitrogen, oxygen and argon is not large (less than the difference between the 4-th and 2-nd approximations for each of the gases).

These theoretical results have been compared with other computations, obtained at the VKI, and with available experimental data in their reliable range for relevant plasmatron temperatures[19].

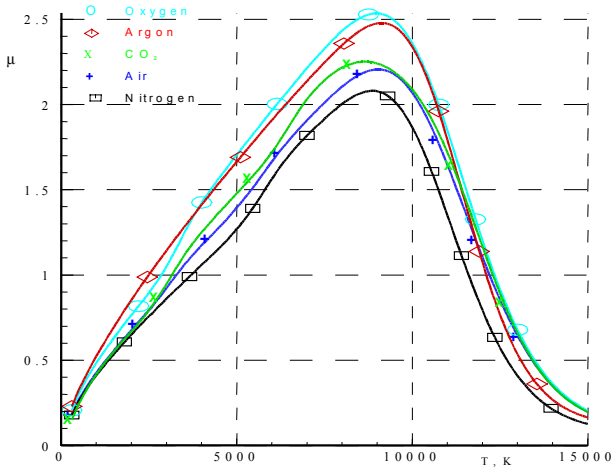

Figure 3.: Viscosity in (Pa*s)/10000 for five gases: air, nitrogen, oxygen, argon and carbon dioxide, calculated in the second non-zero approximation

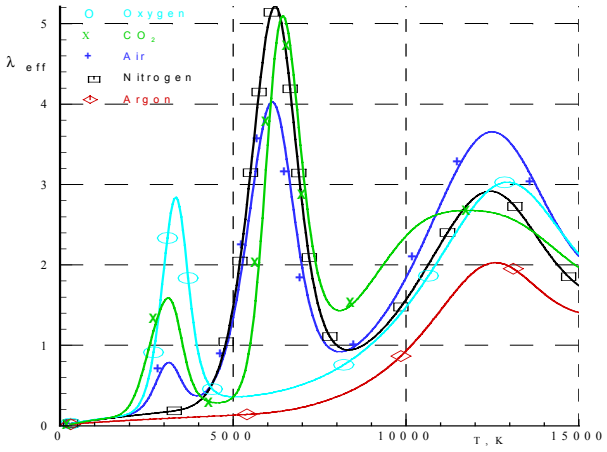

Figure 4.: Effective heat conductivity [W/m/K] for five gases: air, nitrogen, oxygen, argon and carbon dioxide, calculated in the third non-zero approximation

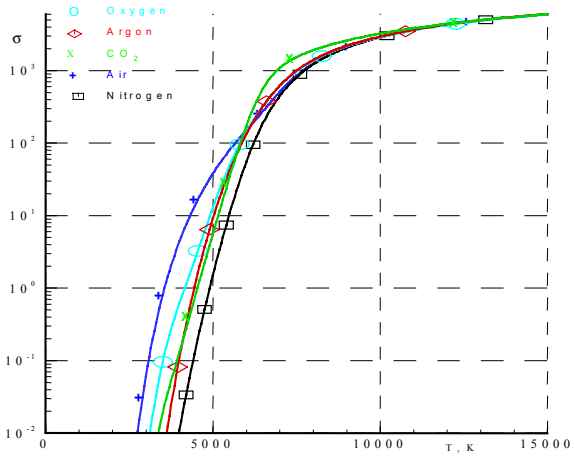

Figure 5.: Electrical conductivity [1/Ohm/m] for five gases: air, nitrogen, oxygen, argon and carbon dioxide, calculated in the third non-zero approximation

6 ICP FLOW SIMULATION RESULTS

Calculations of equilibrium air, nitrogen, oxygen and argon plasma flows for IPG4 discharge channel geometry[13] with the channel radius $R_c = 0.04$ m and length $Z_c = 0.46$ m were performed. The finite-volume method, based on the implicit TVD Harten-Yee scheme[11], and SIMPLE algorithm of Patankar and Spalding along with the under-relaxation procedure to increase stability were used to solve the Navier-Stokes equations. A nonuniform grid spacing of 103 by 43 cells in the axial and radial directions was used in the calculations. The value of RF inductor current is determined in the solution process while the power input in plasma N_{pl} is specified.

Calculations for the five gases were carried out for the single plasmatron operating regime: gas flow rate G = 2.8 g/s with 45 degrees inlet swirl, pressure P = 0.1 atm, $N_{pl} = 20$ kW, frequency f = 1.76 MHz. The wall temperature of both the quartz tube and surface of the gas injector interface was $T_w = 300$ K. Fig. 6 shows the computed streamlines and temperature fields within the IPG-4 discharge channel for air. In the Fig. 7, the profiles of temperature $T(Z_c, r)$ at the channel exit section are presented for the five plasmas. Argon temperature profile is much higher than that of other gases. The very low effective heat conductivity of argon plasma leads to essential difference in temperature field within the channel temperature and the maximum for argon plasma is shifted essentially from the axis to the wall and temperature gradients within “fire ball” are much lower than that for the molecular gases.

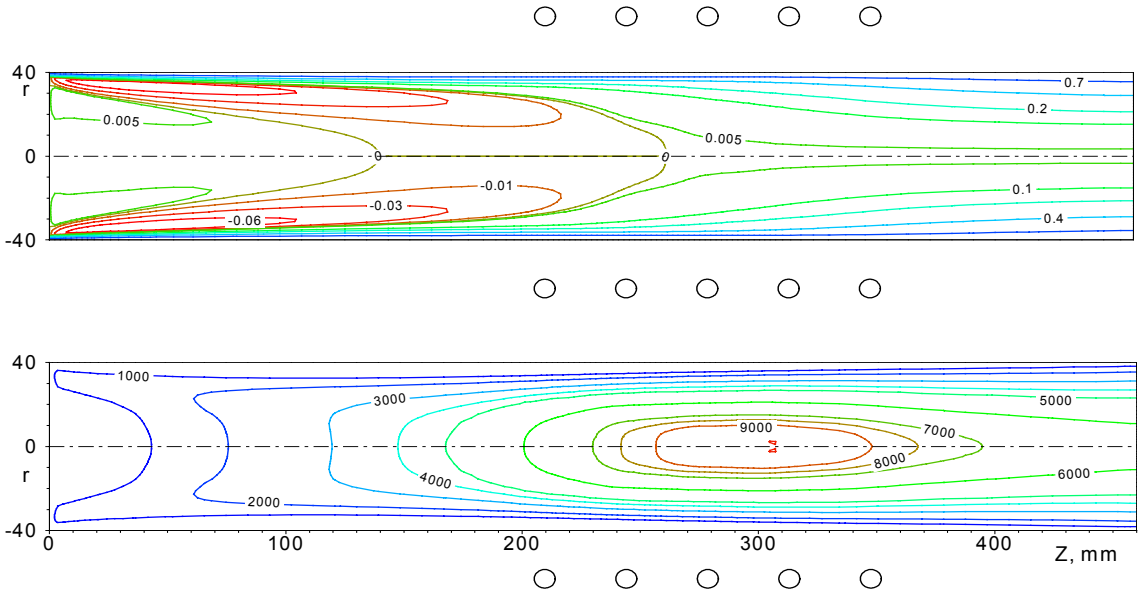

Figure 6.: Streamlines and isotherms for IPG-4 air plasma at P=0.1 atm, G=2.8 g/s, Npl=20 kW, f=1.76 MHz

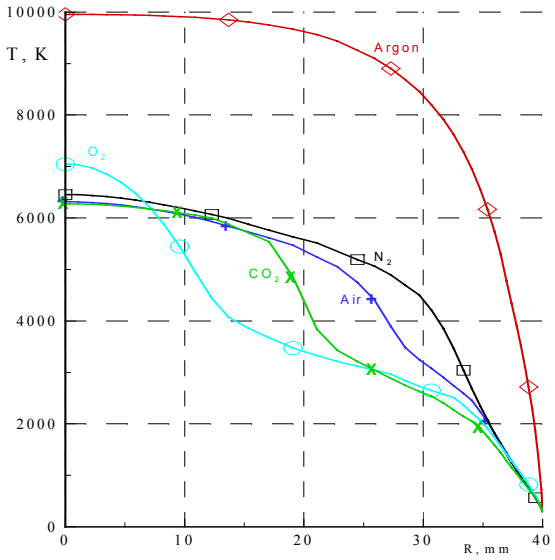

Figure 7.: Temperature T [K] at IPG-4 channel exit section for five gases: air, nitrogen, oxygen, argon and carbon dioxide

The supersonic outflow from the IPG-4 plasmatron through a Laval nozzle into the test

chamber was considered also. The input parameters of the problem are as follows: gas is air, the enthalpy of the injected gas and gas on the wall is kJ/kg, the angle of the flow spinning is 45^0, the operation frequency is 1,76 MHz, power is 20 kW, the consumption of the injected gas is $2{,}8*10^{-3}$ kg/s. Pressure was set 1300 Pa on the subsonic outlet boundary in the test chamber. Thus, rarefaction was created in the test chamber. Mach numbers are changed from $2*10^{-2}$ in the circulated flow up to 2,5 on the nozzle end. In the Fig. 8, the upper part corresponds to streamlines, the lower part – the enthalpy distribution. The pressure was about 700 Pa on the nozzle end. Thus, the jet is overexpanded in this case and the outflow is accompanied by the typical system of shocks and rarefaction waves. A flow pattern near the nozzle, including the first two "casks", is presented in the Fig. 9 by the distribution of pressure. The maximal velocity was about 3000 m/s in the example. All calculations were performed by the unique manner without dividing into different parts.

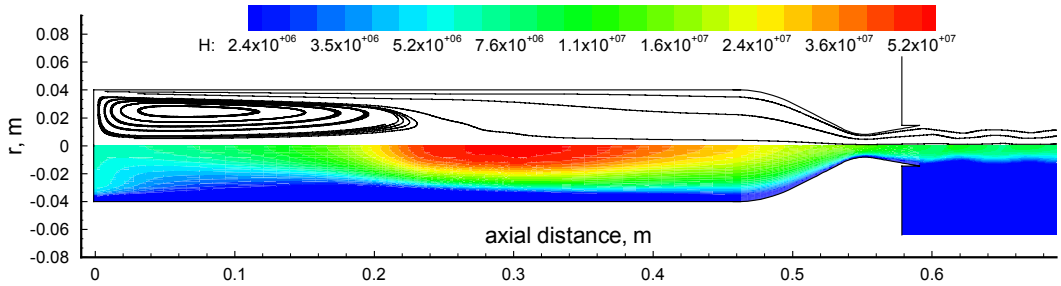

Figure 8.: Supersonic outflow from IPG-4 plasmatron. The upper part corresponds to streamlines, the lower one – enthalpy distribution

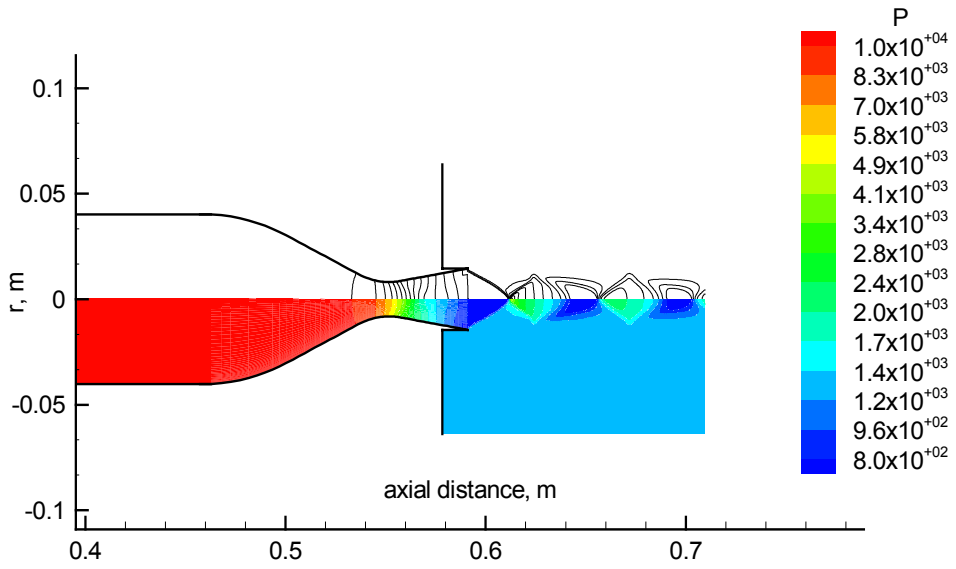

Figure 9.: Outflow into test chamber. Pressure distribution (Pa)

7 CODE-TO-CODE VALIDATION

A comparison of results obtained by three absolutely different codes was done for several operating pressures (1; 0.1; 0.04 atm) in the case of argon. We used the codes mentioned above (code 1 and 2). As well, we present the results[15] obtained at the Von Karman Institute using the code described in[7]. The results obtained by all codes are in a reasonably good agreement. Flow geometry, boundary conditions, mesh are the same as above. The examples of such a comparison are presented in Fig. 10-12. Operating parameters are as follows: the consumption is 2.8 g/s, the operating pressure is 0.1atm, the operating power: 15 kW.

Temperature profiles at axial positions x = 15 sm (inlet region), 27 sm (mid-coil), and 46 sm (outlet) are presented in Fig. 10. Temperature fields and flow structures for both MIPT and IPM results are presented in Fig. 11-12. The similar agreement of the computational results is observed for other pressure parameters.

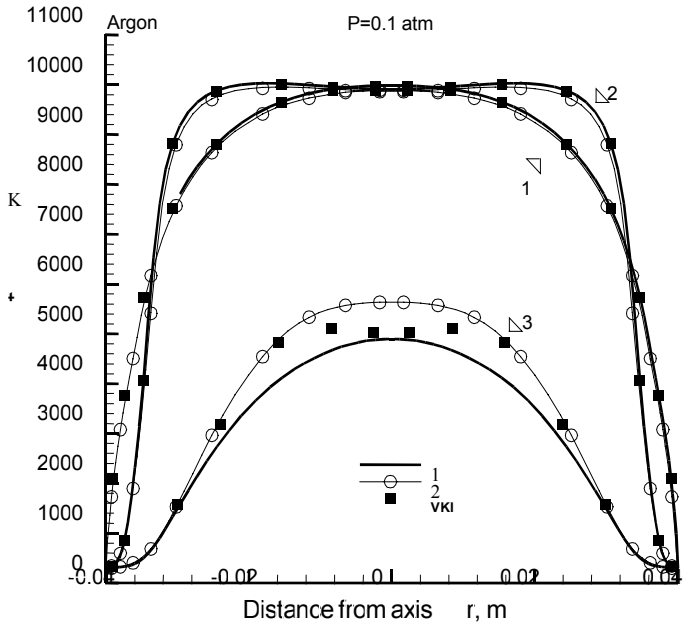

Figure 10: Comparison of temperature profiles at x=15 cm (3), 27 cm (2), and 46 cm (1)

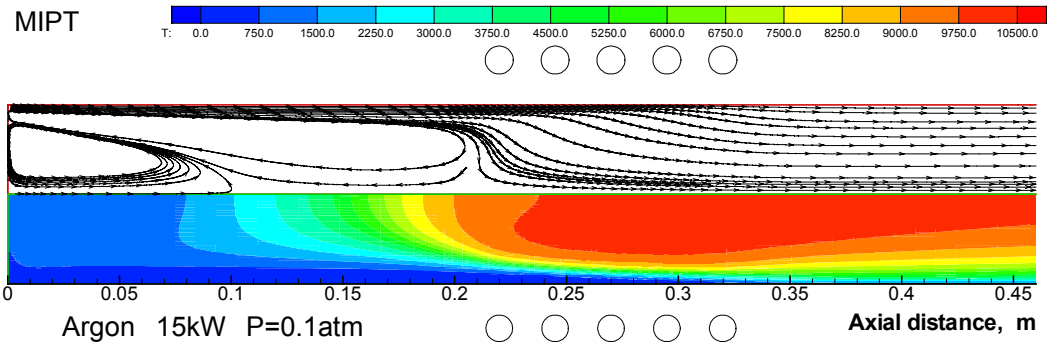

Figure 11.: Temperature field and flow structure in streamlines: code 1 (MIPT)

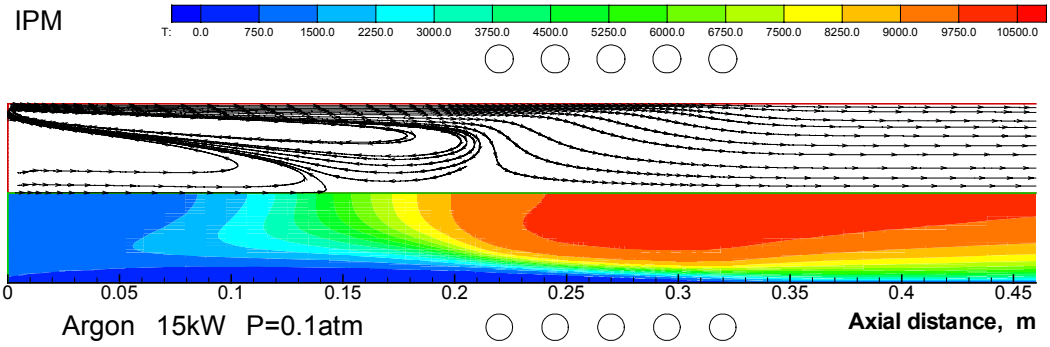

Figure 12.: Temperature field and flow structure in streamlines: code 2 (IPM)

8 CONCLUSION

A physico-chemical model, numerical method and computation results for equilibrium inductive coupled plasma flows in plasmatron were obtained. An advanced technology developed for calculations of the plasma transport coefficients based on the rigorous modification of the Chapman-Enskog formalism and appropriate database for thermodynamic and transport properties are presented.

A new effective preconditioning technique along with an implicit TVD scheme was developed to solve the Navier-Stokes equations in both subsonic and supersonic regimes in a uniform manner. Calculations were performed by the uniform manner without dividing the domain investigated into different parts.

Code-to-code validation was performed for different input parameters. A good agreement takes place for the results obtained by the different computational methods.

9 ACKNOLEDGMENT

This research was supported by the INTAS and RFBR (grants INTAS-RFBR 95-1329, INTAS-ESA 99-01473).

REFERENCES

[1] A.N. Gordeev, A.F. Kolesnikov and M.I. Yakushin, M.I., "An Induction Plasmatron Application to 'Buran's' Heat Protection Tiles Ground Tests," *SAMPE J.*, **28** (3), 29-33 (1992).

[2] A.F. Kolesnikov, "The Aerothermodynamic Simulation in Sub- and Supersonic High-Enthalpy Jets: Experiment and Theory," Proc. of the Second European Symposium on Aerothermodynamics for Space Vehicles, ESTEC, Noordwijk, The Netherlands, November 1994, ESA SP-367, 583-590 (1995).

[3] M. Auweter-Kurtz, F. Hammer, G.Herdrich, H. Kurtz, T. Laux, E. Schreiber and T. Wegmann, "The Ground Test Facilities for TPS at The Institute Fur Raumfahrt-systeme", 3rd European Symp. on Aerothermodynamics for Space Vehicles, ESTEC, Noordwijk, The Netherlands, November 24-26, 1998, ESA SP-426, 529-536 (1999).

[4] B. Bottin, M. Carbonaro, V. Van Der Haegen and S. Paris, "Predicted and Measured Capability of the VKI 1.2 MW Plasmatron Regarding Re-Entry Simulation", 3rd European Symp. on Aerothermodynamics for Space Vehicles, ESTEC, Noordwijk, The Netherlands, November 24-26, 1998, ESA SP-426, 553-560 (1999).

[5] A. Kolesnikov, M. Yakushin, I. Pershin and S. Vasil'evskii, "Heat Transfer Simulation and Surface Catalycity Prediction at the Martian Atmosphere Entry Conditions", AIAA Paper 99-4892 (1999).

[6] A.F. Kolesnikov, I.S. Pershin, S.A. Vasil'evskii and M.I. Yakushin, "Study of Quartz Surface Catalycity in Dissociated Carbon Dioxide Subsonic Flows", *J. of Spacecraft and Rockets*, **37**, 573-579 (2000).

[7] D. Vanden Abeele and G. Degrez, "Numerical Model of High-Pressure Air Inductive Plasmas under Thermal and Chemical Nonequilibrium", *AIAA Paper* 2000-2416 (2000).

[8] A. F. Kolesnikov and G. A. Tirskii, "Equations of Hydrodynamics for Partially Ionized Multi-Component Mixtures of Gases, Employing Higher Approximations of Transport coefficients," (tr. from Russian). In: *Fluid Mechanics-Soviet Research*, Scripta Technica, Inc., **13** (4), 70-97 (1985).

[9] S.A.Vasil'evskii, A.F.Kolesnikov, S.V.Utyuzhnikov, and G.S.R.Sarma, *Physico-chemical Data Base and Computation Results for Inductive Plasma Flows*. In: Progress in Plasma Processing of Materials (Eds. P.Fauchais and J.Amouroux), Begell House, New York, 277- 284, (1999).

[10] C.Viozat, *Implicit Upwind Schemes for Low Mach Number Compressible Flows*, Technical Report 3084, INRIA (1997).
[11] H.C.Yee, R.F.Warming and A.Harten, "Implicit Total Variation Diminishing Schemes for Steady- state Calculations". *J.Comp.Phys*., **57**, (1985).
[12] M.I.Boulos M.I. , Gagne R., Barnes R.M., "Effect of swirl and confinement on the flow and temperature fields in an inductively coupled r.f. plasma", *The Canadian J. of Chemical Engineering*, **58**, 367-381 (1980).
[13] Vasil'evskii S.A., Kolesnikov A.F., Yakushin M.I., Mathematical models for plasma and gas flows in induction plasmatrons, Molecular Physics and Hypersonic Flows, ed. by M.Capitelli, NATO ASI Series, Kluwer, 495-504 (1996).
[14] Makarov B.P., Numerical modeling of high frequency induction discharge in argon. In: Some problems in hydrodynamics, aerophysics and applied mechanics. Moscow, MIPT 49-55 (1985) (in Russian).
[15] D. Vanden Abeele, S. A. Vasil'evskii, A. F. Kolesnikov, G. Degrez, B. Bottin, Code-to-code validation of inductive plasma computations. In: Progress in plasma processing of materials, Eds. P.Fauchais and J.Amouroux, 245-250, Begell House, N.Y., (1999).
[16] S.A.Vasil'evskii, I.A.Sokolova, G.A.Tirsky, "Determination and calculation of transport coefficients for chemically equilibrium partially ionized and fully ionized gas flows", *J. of Applied Mechanics and Technical Physics*. (1) 68-80 (1986) (in Russian).
[17] M.Capitelly, R.S.Devoto, "Transport coefficients of high temperature nitrogen", *Physics of Fluids*, **16** (11), 1835-1841 (1973).
[18] J.H. Ferziger and H.G.Kaper, *Mathematical theory of transport processes in gases*, North-Holland Publ., Amsterdam-London (1972).
[19] B. Bottin, D. Vanden Abeele, M.Carbonaro, G. Degrez, G.Sarma, "Thermodynamic and transport properties for inductive plasma modelling", *J. Thermophys. Heat Transf.*, **13** (3), 443-450 (1999).